

(12)

AD A118723

AFGL-TR-82-0119

ATMOSPHERIC DENSITY MODELS,
INCLUDING TIDES

Jeffrey M. Forbes

Department of Physics
Boston College
Chestnut Hill, Massachusetts 02167

Final Report
28 March 1979 - 28 March 1982

31 March 1982

DTIC FILE COPY

Approved for public release; distribution unlimited

AIR FORCE GEOPHYSICS LABORATORY
AIR FORCE SYSTEMS COMMAND
UNITED STATES AIR FORCE
HANSCOM AFB, MASSACHUSETTS 01731

DTIC
ELECTRONIC
AUG 31 1982
E

02 00 30 148

Unclassified

SECURITY CLASSIFICATION OF THIS PAGE (When Data Entered)

REPORT DOCUMENTATION PAGE		READ INSTRUCTIONS BEFORE COMPLETING FORM
1. REPORT NUMBER AFGL-TR-82-0119	2. GOVT ACCESSION NO. AD-A118723	3. RECIPIENT'S CATALOG NUMBER
4. TITLE (and Subtitle) ATMOSPHERIC DENSITY MODELS, INCLUDING TIDES		5. TYPE OF REPORT & PERIOD COVERED Final Report 28 Mar 1979 - 28 Mar 1982
		6. PERFORMING ORG. REPORT NUMBER
7. AUTHOR(s) Jeffrey M. Forbes		8. CONTRACT OR GRANT NUMBER(s) F19628-79-C-0088
9. PERFORMING ORGANIZATION NAME AND ADDRESS Department of Physics Boston College Chestnut Hill, Massachusetts 02167		10. PROGRAM ELEMENT, PROJECT, TASK AREA & WORK UNIT NUMBERS 62101F 669007AG
11. CONTROLLING OFFICE NAME AND ADDRESS Air Force Geophysics Laboratory Hanscom AFB, Massachusetts 01731 Monitor/Dorothy F. Gillette/LKB		12. REPORT DATE 31 March 1982
		13. NUMBER OF PAGES 15
14. MONITORING AGENCY NAME & ADDRESS (if different from Controlling Office)		15. SECURITY CLASS. (of this report) Unclassified
		15a. DECLASSIFICATION/DOWNGRADING SCHEDULE
16. DISTRIBUTION STATEMENT (of this Report) Approved for public release; distribution unlimited		
17. DISTRIBUTION STATEMENT (of the abstract entered in Block 20, if different from Report)		
18. SUPPLEMENTARY NOTES		
19. KEY WORDS (Continue on reverse side if necessary and identify by block number) Atmospheric temperatures Winds Densities Tides		
20. ABSTRACT (Continue on reverse side if necessary and identify by block number) A numerical model has been developed to solve the linearized atmospheric tidal equations for diurnal and semidiurnal temperatures and the 3 velocity components of the wind field from the surface to the upper thermosphere (Ca. 400 km). Density, pressure, and composition variations can be computed from a simple auxiliary set of equations. Extensive tables and figures have been compiled for potential users. Validity of the model has been verified by comparison with various rocket and satellite data.		

DD FORM 1473
1 JAN 73

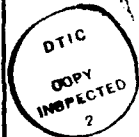
EDITION OF 1 NOV 65 IS OBSOLETE

Unclassified

SECURITY CLASSIFICATION OF THIS PAGE (When Data Entered)

Data analyses performed include (a) seasonal-latitudinal tidal structures of total mass density from the Atmosphere Explorer -C, -D, -E, and Air Force S3-1 satellite accelerometer experiments; (b) a linear regression fit of neutral exospheric temperatures derived from Thomson scatter measurements at Millstone Hill; and (c) satellite densities and Millstone Hill temperatures during the magnetic storm of March 21-22, 1979.

Accession For	
NTIS GRA&I	<input checked="" type="checkbox"/>
DTIC TAB	<input type="checkbox"/>
Unannounced	<input type="checkbox"/>
Justification	
By	
Distribution/	
Availability Codes	
Avail and/or	
Dist	Special
A	



1. THEORETICAL MODELLING

Much of the work involved in the first year of this contract involved development of a numerical model to solve the linearized atmospheric tidal equations from the surface to 400 km. This basically involved modifications of a thermospheric tidal model developed under the previous AFGL Contract F19628-76-C-0059 along the following lines:

1. Development of new parameterizations of eddy and molecular viscosity and thermal conductivity.
2. Development of a model of background winds, temperatures, and composition from the surface to 400 km, and incorporation into the tidal model. Combinations of trigonometric and exponential functions were utilized to obtain analytic descriptions of the background fields for use in the numerical calculations.
3. Derivation of a new set of tidal equations generalized to take into account background winds and meridional structure gradients, and incorporation into the numerical model. In addition, the equations and computer coding were converted from a pressure coordinate system to a stretched altitude coordinate system to facilitate later steps in the analysis and use of the results.
4. Development of new models of UV and EUV heating in the thermosphere, and momentum sources due to correlations between the wind and ion drag components, for the diurnal, semidiurnal, and terdiurnal solar tides.
5. Modification of the empirical ionospheric model developed by Ching and Chiu of the Aerospace Corporation to yield the zonal mean, diurnal, and semidiurnal components of the ion drag coefficient.
6. Incorporation of gravitational forcing for the lunar tide.
7. Development of auxiliary routines to (a) interpolate and synthesize

propagating tides excited by O_3 and H_2O insolation absorption with those excited in-situ in the thermosphere; (b) construct tables for publication as report appendices; (c) plot vertical and horizontal amplitude and phase structures of the computed results.

Extensive computations with the numerical model have resulted, first of all, in two papers which have been accepted for publication in the Journal of Geophysical Research:

"Atmospheric Tides: I. Model Description and Results for the Solar Diurnal Component" by J.M. Forbes.

"Atmospheric Tides: II. The Solar and Lunar Semidiurnal Components" by J.M. Forbes.

In Part I, the equations and boundary conditions governing tidal oscillations in a viscous, rotating, spherical atmosphere from the surface to 400 km are formulated, including model parameterizations of background winds, temperature, composition, hydromagnetic coupling, Newtonian cooling, eddy and molecular diffusion, and tidal forcing mechanisms. Excitation of the tidal oscillations is assumed to occur via absorption of EUV and UV radiation in the thermosphere, H_2O insolation absorption in the troposphere and lower stratosphere, O_3 insolation absorption in the mesosphere, ion-neutral momentum coupling in the F-region, and lunar gravitational forcing. The method of solution for the equations is outlined, and numerical convergence of the viscous model for certain test cases is verified by comparison with analytic calculations below 100 km from classical (inviscid) tidal theory.

In addition, calculated results for the solar diurnal tide from the surface to 400 km are presented and compared with rocket and radar observations. Considering the day-to-day variations which are clearly evident in the data, observations of tides by various rocket and radar techniques are

in good agreement with the "mean tidal structures" represented by the model. The greatest inconsistencies occur in the 80-100 km height region where the diurnal propagating tide and the in-situ trapped tide are of comparable importance at midlatitudes. The (1,1) propagating tide above 70 km is sensitively coupled to the intensity of turbulence in the tropical mesosphere as parameterized by the eddy coefficients for diffusion of momentum and heat, undoubtedly contributing to its vagarious nature.

In an effort to explain apparent asymmetries about the equator of diurnal tidal variations in winds and temperatures between 40 and 110 km derived from rocket campaigns at two geographically-conjugate stations (Natal, 5.9°S; Kourou, 5.1°N), an attempt has been made to simulate these data theoretically by introducing the first antisymmetric diurnal propagating tidal mode (1,2), in addition to the well-known symmetric (1,1) mode. The (1,2) mode is shown to be capable of adequately explaining the amplitude and phase difference between the temperature oscillations at both stations. However, the calculated asymmetries in the westerly and southerly velocities are completely inconsistent with the observations, thus precluding this explanation of the data. Remaining possibilities to explain these differences include:

- a. Longitudinal variations in the tides and other atmospheric properties.
- b. Day-to-day variability of diurnal tides, possibly induced by changing eddy diffusivities.
- c. Mode "distortion" rather than mode "coupling" induced by background mean winds. In other words, the asymmetric behavior might be better explained by a distorted (1,1) mode due to asymmetric mean winds, rather than coupling into the (1,2) mode.
- d. The attempted interpretation of global data sets taken during

non-overlapping time periods.

In Part II, solar and lunar semidiurnal wind and temperature oscillations from the surface to 400 km are simulated for average solar activity conditions utilizing the numerical tidal model described in Part I. Hough mode decomposition of the solstitial solar semidiurnal tide excited by H_2O and O_3 insolation absorption below 80 km indicates that it is characterized by a predominance of (2,2) below 60 km; about equal contributions of (2,2), (2,3), and (2,4) between 70 and 90 km; mostly (2,4) with some (2,5) and (2,2) between 90 and 120 km; and predominance of (2,2) above 140 km with secondary contributions from (2,3), and (2,5) between 80 and 110 km; and by (2,2) with a fairly strong secondary contribution from (2,3) above 120 km. Similar descriptions for both the solar and lunar oscillations apply at equinox, except that the asymmetric (2,3) and (2,5) modes are absent. Relative to the solar component, lunar temperature and wind amplitudes are sufficiently large (~20%) in the lower and upper thermosphere to account for some of the observed variability previously attributed to the solar tide. Amplitudes of the (2,4) and (2,5) modes above 100 km are significantly affected by mesospheric eddy diffusion coefficients in excess of $2 \times 10^6 \text{ cm}^2 \text{ sec}^{-1}$. The total solar semidiurnal exospheric temperature oscillation for average solar conditions ranges from ~10-20 K poleward of 40°N to ~40-60 K equatorward of 30°N , and has its origin in three sources of excitation all of comparable importance: (1) EUV solar radiation absorption in the lower thermosphere (100-200 km); (2) in-situ momentum coupling due to the interaction of diurnal winds and diurnally-varying ion drag; and (3) tides propagating upwards from below 100 km. In addition, the calculations are compared with rocket, meteor radar, partial reflection, Thomson scatter, and satellite data to evaluate the consistency of the model with observations.

Due to the volume of material covered by the above studies, only results at select latitudes for equinox conditions are illustrated along with some comparisons with observational data. Therefore, an AFGL Report entitled "A Compendium of Theoretical Atmospheric Tidal Structures. Part I. Explicit Structures due to Realistic Thermal and Gravitational Excitation" by J.M. Forbes and D.F. Gillette has been constructed which details the tidal equations, numerical method of solution, and model parameterizations, and presents extensive tables and figures of all numerical results for the diurnal and semidiurnal tides as summarized and described in the two JGR articles referred to above.

In the course of the model development and calculations, the electric field model of A.D. Richmond (NOAA/ERL) has been incorporated into the thermospheric tidal model to evaluate the effects of electric field-driven plasma drifts on the tidal dynamics of the neutral thermosphere. Calculations show that no more than a 12% increase in the neutral zonal wind can be generated by momentum transfer from the ionospheric plasma during geomagnetically quiet periods at the equator. The increase is somewhat smaller at mid-latitudes. Richmond's model only extends to 60° latitude and this does not include the important high latitude regions. The effect is more likely to assume more significance at high latitudes or during geomagnetic disturbances and will be examined when plasma drift models of the high latitude and magnetically disturbed ionosphere are available.

In a related effort, the model (with background winds and meridional temperature gradients set equal to zero) was utilized to calculate the extensions into the thermosphere of normalized wind and temperature structures associated with the (2,2), (2,3), (2,4), and (2,5) semidiurnal propagating tidal modes. The structures can be used, for instance, to extend

meteor wind (80-100 km) and partial reflection drift (60-100 km) measurements to heights above 100 km for consistency checks with tidal winds and temperatures from Thomson scatter measurements, possibly at different latitudes, or to simultaneously fit data covering these height regions for modelling purposes. A summary version of these results (with additional figures plus tables available on microfiche) is contained in a JGR article which has been accepted for publication:

"Thermospheric Extensions of the Classical Expansion Functions for Semidiurnal Tides" by J.M. Forbes and M.E. Hagan.

An expanded version of this work has been prepared as an AFGL report entitled "A Compendium of Theoretical Atmospheric Tidal Structures. Part II. Thermospheric Extensions of the Classical Expansion Functions for Semidiurnal Tides" by J.M. Forbes, M.E. Hagan, E. DiCesare, and D.F. Gillette. In this report figures are presented which illustrate the degree of alteration of vertical tidal structures with latitude, and the change in horizontal shapes with height, corresponding to semidiurnal oscillations in northerly, westerly and vertical velocity, and temperature in the thermosphere. Figures and tables covering the 80-400 km altitude region for five levels of solar activity at 6° latitude increments constitute the Appendix of this report.

A summary of results from the two-part JGR article and their interpretation was presented at the Spring 1981 AGU Meeting in Baltimore, Maryland. In addition, an invited review paper entitled "Tides in the Thermosphere: A Review" by J.M. Forbes was presented at the August 1981 IAGA Meeting in Edinburgh, Scotland. In this review recent theoretical and observational accomplishments relating to diurnal and semidiurnal tidal oscillations of neutral winds, temperature, density, and composition above 100 km were presented. Topics emphasized included: (1) Recent theoretical

studies; (2) Solar cycle, seasonal, and latitudinal variations in tidal oscillations of temperature and winds as inferred from Thomson scatter measurements; (3) Tidal variations in total mass density and composition as inferred from satellite accelerometer and mass spectrometer measurements; (4) Comparison of recent theoretical models with the above observations; (5) The relative influence of in-situ and propagating tides in determining the total semidiurnal thermospheric tide; and (6) Propagating tides of lower atmosphere origin as a source of mean momentum and heat in the lower thermosphere. A shortened version of this talk was also presented at the October 1981 NASA/Goddard Workshop on Thermospheric Dynamics.

2. DATA ANALYSES

The seasonal-latitudinal tidal structures of O, N₂, and total mass density in the thermosphere for minimum and maximum levels of solar activity were investigated using a theoretical model and accelerometer data from the Atmosphere Explorer-C, D, -E, and Air Force S3-1 satellites. The 45,298 data points analyzed cover latitudes between 0° and 80°, altitudes between 145 and 245 km, and 24 hours in local time. According to the theory, oxygen variations are strongly influenced by seasonal differences in the winds, whereas N₂ responds primarily to temperature which has a different seasonal dependence than the winds. The tidal variation of total mass density is complicated by its dependence on the relative amplitudes and phases of the O and N₂ variations. The net effect is that rather complicated and different seasonal-latitudinal tidal structures are predicted to occur. The theoretical height structures of diurnal amplitude and phase of O, N₂, and total mass density during solar minimum near the equator were found to be in good agreement with recently published Atmosphere Explorer-E experimental data. As

a result of the analysis of accelerometer-derived densities, the predicted shift to later local times from the equator to midlatitudes of the diurnal phase of total mass density has been verified. This effect is basically a manifestation of the relative amplitudes and phases of O and N₂ variations at different latitudes, which are in turn controlled by the relative influences of tidal winds and temperature in determining tidal changes in composition. A manuscript describing the above work entitled

"Seasonal-Latitudinal Tidal Structures of O, N₂, and Total Mass Density in the Thermosphere" by J.M. Forbes and F.A. Marcos

was published in the Journal of Geophysical Research (83, 3489-3493, 1980). This work was also presented at the Spring 1979 AGU Meeting in Miami, Florida.

Data analyses performed during this reporting period have also involved Millstone Hill (MH) exospheric temperature data provided by Dr. R. Oliver, MIT Lincoln Laboratory. These data consist of 3,012 temperatures at 300 km covering 181 days between 1969 and 1975, and were derived from the more accurate "two pulse" experiments at MH. Less accurate data from the 1969-1971 time period were analyzed and compared to St. Santin data by Salah et al (1976)(Ann. Geophys. 32, 257-266), and represent a major portion of the incoherent scatter data base for the MSIS model. Three approaches were used to apply the method of multiple linear regression and to determine an expression for exospheric temperature of the form:

$$\begin{aligned}
T_{\infty} &= A_0 + A_1 \Delta F + A_2 (\Delta F)^2 + A_3 \bar{F} + A_4 \Delta A_p + A_5 \cos \Omega (d - d_{10}) \\
&+ A_6 \bar{F} \cos \Omega (d - d'_{10}) + A_7 \cos 2\Omega (d - d_{20}) + A_8 \bar{F} \cos 2\Omega (d - d'_{20}) \\
&+ A_9 \cos \omega (t - t_{1\max}) + A_{10} \bar{F} \cos \omega (t - t'_{1\max}) + A_{11} \cos 2\omega (t - t_{2\max}) \\
&+ A_{12} \bar{F} \cos 2\omega (t - t'_{2\max}) \\
t_{1\max} &= t_{10} + t_{11} \cos \Omega (d - d_{11}) \\
t_{2\max} &= t_{20} + t_{22} \cos \Omega (d - d_{22}) \\
\Omega &= 2\pi / 365 \text{ day}^{-1} \quad \omega = 2\pi / 24 \text{ hour}^{-1} \\
\Delta \bar{F} &= \bar{F}_{10.7} - 150 \\
\Delta F &= \bar{F}_{10.7} - F_{10.7} \\
\Delta A_p &= A_p - 4 \\
d &= \text{day of year} \\
t &= \text{local time}
\end{aligned}$$

Method 1:

Individual days of data with 24 hour coverage were analyzed separately to determine the daily mean, diurnal, and semidiurnal components. The amplitudes and phases of the diurnal and semidiurnal components were then fitted with functions representing the seasonal and solar cycle variations of these quantities. The mean component was similarly analyzed to yield the geomagnetic, solar flux, and semiannual variations in the daily mean temperature. These results were combined to yield a representation for the exospheric temperature as given above. One disadvantage of this method is

that adequate coverage over 24 hours local time is required for each day analyzed; thus, data taken during days of spotty radar coverage had to be omitted from analysis.

Method 2:

The data were also analyzed by fitting a single equation of the form given above to all 3,012 data points. Coefficients obtained from applying this procedure are tabulated in Table I, which resulted in a correlation coefficient of 0.84.

TABLE I
Coefficients Obtained from Linear Regression Analysis
of all 3,012 Data Points

	<u>MSIS</u>	<u>Current Analysis</u>
A ₀	1008	1101
A ₁	1.25	1.95
A ₃	3.33	3.76
A ₄	8.54	4.10
A ₅	79.3	38
A ₆	.51	.51
A ₇	3.3	10.9
A ₈	0	.23
A ₉	118	54
A ₁₀	.66	.93
A ₁₁	27.5	29
A ₁₂	.15	.4

Differences between the current analysis and the MSIS coefficients are largely due to (a) The use of more accurate 2-pulse data in the present analysis,

whereas the MSIS model is based on the less accurate and uncorrected 1-pulse data; and (b) Inadequate solar cycle coverage in the 1970-1975 set.

Method 3:

It is anticipated that eventually so many data points will be available for analysis that a regression analysis of all data points at once might be precluded by computer limitations. Also, it was felt that another alternative method of data analysis would benefit our understanding of the variations in the data. A third method was developed whereby data points were separated into $F_{10.7}$ bins (60-80; 80-100; 100-120; 120-140; 140-160; 160-180), and within each bin the data points were fitted with mean, diurnal, semidiurnal, seasonal, semiannual, and geomagnetic activity terms. Then, the amplitudes of these terms were looked at as a function of $F_{10.7}$ to extract any solar cycle dependence of these variations.

It was found that examining the data in 3 ways greatly assisted in the understanding of variations in the data, and made clear pitfalls in a straightforward multiple linear regression analysis of all the data (Method 2). For instance, Method 2 indicated a solar cycle variation of the diurnal amplitude of $184 + 2.7 \Delta \bar{F}$. Although this represents a best fit to the data currently available, based on other data analyses (Method 1; MSIS model) and theoretical calculations by this investigator, the slope of this line is much too high to be realistic. Basically, better coverage at high solar activity levels is required before this variation is adequately modelled. Also, solar cycle variations in seasonal amplitudes must be suspect, since yearly coverage is inadequate at various levels of solar activity. Future work along these lines planned for the subsequent AFGL contract involves extending the data set to include the recent solar maximum (1978-1982), improving the seasonal and magnetic activity coverage, and performing similar analyses with Arecibo

(18°N) exospheric temperatures.

Accelerometer data obtained from F.A. Marcos for the March 21-22, 1979, time period, have been normalized to 200 km and plotted vs time at -40°, -20°, 0°, 20°, 40°, 60°, 65°, 75°, and 85° latitude for day (~ 1000 LT) and night (~ 2200 LT) conditions, and examined to ascertain the thermospheric response to the geomagnetic storm occurring during this period. The data illustrate that the daytime thermospheric response to geomagnetic activity at high latitudes exceeds that at nighttime, whereas a tendency towards the opposite behavior occurs equatorward of about 40-60° latitude. These data should be further studied by examining the latitude structures at various times during the storm period, again comparing day and night conditions, but efforts were temporarily curtailed due to lack of resources. It is planned to continue interpretation of these measurements as part of the subsequent contractual effort.

In conjunction with the analysis of satellite density measurements described above, a preliminary analysis of Millstone Hill exospheric temperature data during the March 21-22, 1979, magnetic storm period has been performed. Temperature values for this time period were computed according to the following procedure:

1. T_e , T_i , N_e were derived from measured autocorrelation spectra at heights between 250 and 450 km.
2. T_n values were determined from T_e , T_i , N_e by solving the heat balance equation.
3. Hourly means of T_n were taken to remove statistical fluctuations.
4. The "quiet-day" variation was inferred by fitting a curve to the first 20 hours of data, and extrapolating this fit into the last 16 hours of data.

5. The "quiet-day" variation was then removed from the measured temperatures to infer the variation associated with magnetic storm activity during the second day.

The resulting curve clearly illustrates a ~ 200 K response to the Kp increase from 1⁻ to 7⁻ with a time delay on the order of an hour. A more complete analysis of these data, again scheduled for the subsequent contractual effort, will utilize an electron density calibration procedure which has recently been developed at Millstone Hill, and a more accurate description of the "quiet day" diurnal variation.